Nature Environment and Pollution Technology
An International Quarterly Scientific Journal

ISSN: 0972-6268	Vol. 15	No. 3	pp. 833-840	2016

Original Research Paper

Effect of Construction Dust on Urban $PM_{2.5}$ Emission Characteristics: A Case Study of the Main Urban Area of Chongqing, China

Du Yongjie*, Ren Hong*, Cai Weiguang*, Qin Beibei and Ma XianRui***
*School of Construction, Management and Real Estate, Chongqing University, Chongqing, 400045, China
**School of Build Environment, University of Reading, Reading, RG6 6AW, United Kingdom
†Corresponding author: Ren Hong

Nat. Env. & Poll. Tech.
Website: www.neptjournal.com

Received: 10-05-2016
Accepted: 21-06-2016

Key Words:
Construction dust
$PM_{2.5}$ emission
AERMOD Model

ABSTRACT

This paper attempts to accurately evaluate the contribution of construction dust to China's $PM_{2.5}$ emissions in order to increase environmental authorities' efficiency at managing emissions in urban environments. The study was conducted in the main urban area of Chongqing. Three typical construction sites were designated as the study area, where $PM_{2.5}$ emission concentration data were collected through field investigation and processed by an AERMOD model. $PM_{2.5}$ emission intensity and annual average $PM_{2.5}$ emissions from construction dust in the study area were also ascertained. The results showed that the $PM_{2.5}$ emission intensity and annual average $PM_{2.5}$ emissions from construction dust in the study area were 0.0059 kg/m^2 month and 6220.5 t, respectively. The $PM_{2.5}$ emission concentration of construction dust showed a negative correlation with real-time wind speed. This paper's conclusions can serve as a reference for related departments that make decisions on $PM_{2.5}$ emission management.

INTRODUCTION

Construction dust refers to dust raised by construction sites (e.g. urban infrastructure construction, architecture building and demolition, plant engineering, decoration and repair projects) and construction processes (SIK et al. 2009). It is produced by human activities at construction sites, moves with air flow, and turns into micro-particles (mainly $PM_{2.5}$). More specifically, the activities of construction workers or the operation of machines produces abundant dust which suspends in the air, lowering the air quality (Chang et al., 2010). Construction dust is an ideal carrier of bacteria and viruses due to its strong absorptivity, contains many elements (C, H, O, S, Cl, Fl), and is highly toxic (Huang et al. 2010). It causes various diseases and can be life-threatening if it enters lungs (Santacatalina et al. 2010). It also negatively influences the growth of surrounding plants (Su et al. 2010). Moreover, construction dust significantly reduces visibility. Research has demonstrated that in most cases, light scattered by microparticles (especially particles smaller than 2.5μm) is the main cause of low visibility in urban areas (Kong et al. 2011). Construction dust also causes buildings' and municipal facilities' paint to fade by adhering to it, destroying the urban landscape and visual perception (Wang et al. 2012). Clearly, better control of construction dust and its pollution damage have become urgent problems for the fields of architecture, construction and environmental protection.

Construction dust is a major source of particles and contributes greatly to the PM_{10} and $PM_{2.5}$ in the atmospheric environment (Ni et al. 2012). The production of construction dust is closely related to the construction environment and also strongly correlates with weather conditions, particularly wind speed (Huang et al. 2012). Choosing appropriate monitoring indexes after investigating the emission and pollution characteristics of construction dust is significant for controlling pollution and the improvement of urban air quality (Kim 2015). Many scholars have studied construction dust. Zhao et al. (2007) conducted a study on construction dust and its control in Beijing and established an ARPS Models-3 coupling model system. They found that the greatest contributions of construction dust to air pollution in Beijing were made in January, April, August and October, representing 8.82%, 8.25%, 12.14% and 13.74%, respectively. Wang et al. (2007) analysed the size distribution of unorganized emission particles in Beijing and determined their mass percentages. They concluded the size distribution to be 0-100μm particles. Inhalable particles had the highest mass percentage in urban dust (16.26%); the median diameter D_{50} was the smallest (34μm), and fine particles had the highest content. Wen (2011) conducted a numerical simulation of the spatial migration pattern of urban construction dust by using the Euler-Lagrange stochastic trajectory model and the Monte Carlo mathematical simulation method, disclosing the spatial migration law of urban dust. Tian et al. (2008) studied the spatial diffusion of urban construction dust and explored the vertical diffusion law of construction dust at the boundaries of construction sites. They also examined the horizontal diffusion law of construction dust by detecting variations of dust concentration at different positions of the same height within a 0-200m radius from the construction site. They completed the vertical and horizontal diffusion model of construction dust through data regression. Based on collected data on PM_{10}, $PM_{2.5}$, weather, road dust, and vehicle quantity, Zhao et al. (2009) established a quantitative model of construction dust-induced PM_{10} and $PM_{2.5}$ emission factors by using the FDM model and determined the main influencing factors of construction dust emission. Using the United States' EPA's AP-42 method and related methods of Taiwan's EPA, Huang (2006) corrected the formula parameters for road dust, Junkyard dust, and construction dust in Shanghai and Wusongjiang Industrial Park. He then estimated the amount of dust by combining collected data and field investigations. The spatial distribution characteristics of dust in Shanghai were determined by using a spatial statistical approach. Han et al. (2011) discussed the contributions of construction dust to the concentration of $PM_{2.5}$ in the atmospheric environment of Hong Kong. Querol et al. (2004) analysed the contributions of construction dust to the concentration of $PM_{2.5}$ in Spain.

Chinese research into ground dust has focused on emission and diffusion laws as well as chemical analysis. Few have calculated the total $PM_{2.5}$ produced by construction dust. This paper addresses the gap in the literature by discussing $PM_{2.5}$ emission intensity and total $PM_{2.5}$ emissions produced by construction dust.

MATERIALS AND METHODS

Existing methods for estimating construction dust include division of the underlying surface type and the AP-42 method of the United States' EPA. The first two methods have poor estimation accuracy and do not grade sizes (Chang et al. 2014). The AP-42 method estimates regional emissions, emissions of specific equipment, and emissions related to the surrounding air quality. The AP-42 formula for estimating dust emissions is an empirical formula gained from regression analysis of numerous emission tests. This is currently the sole method accepted worldwide. The United States' EPA released the *Compilation of Air Pollutant Emission Factors* (AP-42) in 1972 and has regularly added new content. The formula discussed in this paper is from the AERMOD (AMS/EP REGULATORY MODEL) model in the 5th edition of AP-42.

The AERMOD model is a steady-state plume model. It is rooted in the statistical theory of diffusion and established with Gaussian diffusion formula. It hypothesizes that pollutant concentration distribution conforms to a normal distribution within a certain range (Tartakovsky et al. 2013). In a steady boundary layer, it portrays horizontal and vertical concentration distribution as Gaussian. In a convective boundary layer, the horizontal concentration distribution is also regarded as Gaussian, but the vertical concentration distribution is described as a double-Gaussian probability-density function (Frost 2014).

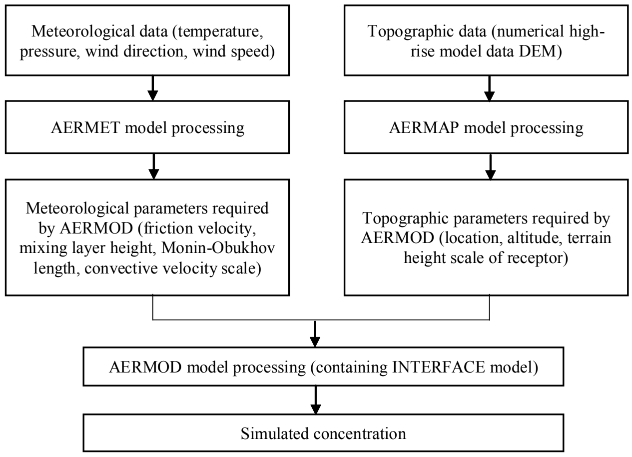

Fig.1: Theoretical framework of AERMOD model.

Composition and principle of AERMOD model: The AERMOD modelling system is an integrated system which includes AERMOD Meteorological Preprocessor (AERMET), AERMIC Dispersion Model (AERMOD), and AERMOD Terrain Preprocessor (AERMAP) (Gulia et al. 2015). The theoretical framework of the AERMOD system is shown in Fig. 1.

Basic computational formula using the AERMOD model: The AERMOD model uses the concept of dividing the streamline to discuss the effect of terrain (including ground barriers) on pollutant concentration and distribution. The diffusion flow field is divided into two layers. The critical shunting height (Hc) is defined as Equation (1):

$$\frac{1}{2}u^{2\circ}\{H_c\} = \int_{H_c}^{h_c} N^{2\circ}(h_c\text{-}z)dz \qquad ...(1)$$

Where, Hc is the kinetic energy of high fluid. The bottom flow field bypasses barriers horizontally while the upper flow field crosses barriers. Concentration at any grid point is the weighted sum of these two plume concentrations.

Suppose the mass concentration formula of a grid point $\{X_{r\ddot{y}}Y_{r\ddot{y}}Z_r\}$ when the influence of terrain is neglected is C $\{X_{r\ddot{y}}Y_{r\ddot{y}}Z_r\}$. The total mass concentration (C_T) when terrain influence is considered as Equation (2):

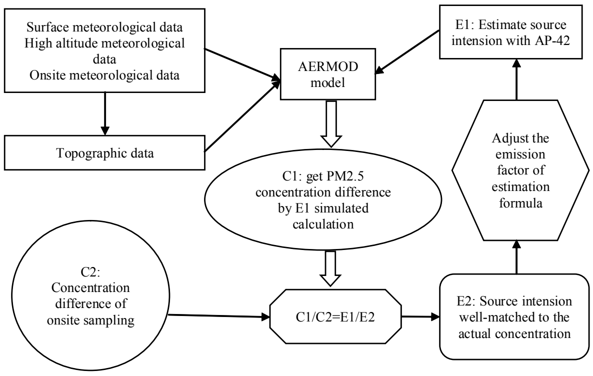

Fig. 2: Modification idea of AERMOD model for estimating PM2.5 emissions.

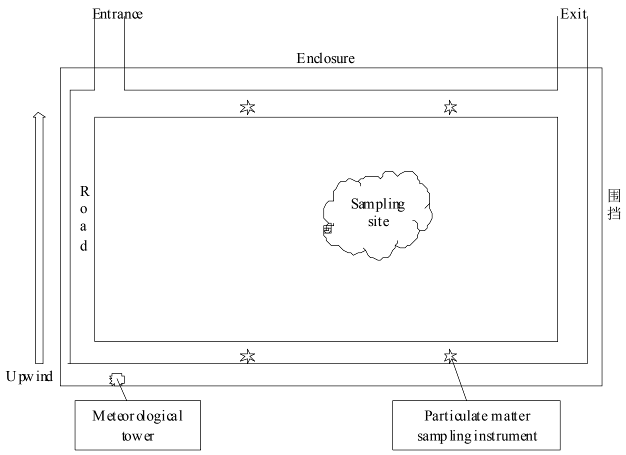

Fig. 3: Detection of upwind and downwind concentrations.

$$C_T\{X_r,Y_r,Z_r\} = f°C\{X_r,Y_r,Z_r\} + (1-f)°C\{X_r,Y_r,Z_p\} \quad ...(2)$$

Where, CT{xr , yr , zr} is the expression of total concentration; zp is the effective height of point (xr, yr, zr), expressed as zp =zr –zt (zt is altitude of the point); f is the weight function of two plume states and determines the degree of influence terrain has on concentration calculations. When f=1, concentrations of all grid points are calculated as diffusion on flat terrain. f is determined by atmospheric stability, wind speed and plume height relative to the terrain. Under stable conditions, the horizontal plume takes the dominant role and is given greater weight. Under neutral and unstable conditions, lifting plumes along the terrain are given greater weight. The plume mass/total plume mass under Hc (φp) has to be calculated before calculating f (Equation 3).

$$\varphi_p = \frac{\int_0^{h_c} C\{X_r,Y_r,Z_r\}dz}{\int_0^{\infty} C\{X_r,Y_r,Z_r\}dz} \quad ...(3)$$

Then, φ_p can be substituted into Equation (4) to calculate f:

$$f = \frac{1}{2}\{1+\varphi_p\} \quad ...(4)$$

The general expression of total mass concentration as Equation (5):

$$C\{X_r,Y_r,Z_r\} = \frac{Q}{u} p_y\{Y, X\} p_z\{Z, X\} \quad ...(5)$$

Where, Q is the discharge rate of the emission source, ū is effective wind speed, and $p_y\{y, x\}$ and $p_z\{z , x\}$ are probability density functions of horizontal and vertical concentration distributions.

AERMOD modified model for estimating $PM_{2.5}$ emissions: Fig.2 shows the idea for modifying the AERMOD model to estimate $PM_{2.5}$ emissions. E_1 can be calculated directly by combining the estimation formula of the AP-42 method and field sampling analysis. C_2 is the difference of field monitoring concentrations (downwind concentration minus upwind concentration). C_1 is the difference between upwind and downwind concentrations as simulated by the Gaussian model (downwind concentration minus upwind concentration). E_2 is the new pollution emission intensity which is gained from the modified formula. The detection principle of upwind and downwind concentrations during field sampling is shown in Fig. 3.

According to the empirical formula in the 5^{th} edition of the AP-42 method, the emission source (construction site) data and related emission parameters are necessary to estimate construction dust emissions. In this paper, construction site conditions in the urban area of Chongqing in November, 2015, from the Chongqing Construction Quality Supervision Network, were used as emission source data. The data covers 1,793 construction sites totalling 131,799,107 m^2 of land. Construction areas in different administrative districts in 2015 are shown in Table 1. Main distributions are marked by red dots in Fig. 4.

Construction dust emissions were estimated using Equation (6):

$$EC=A×T×EFC \quad ...(6)$$

Where, EC represents particulate emissions from construction sites (tons/year), A represents construction areas

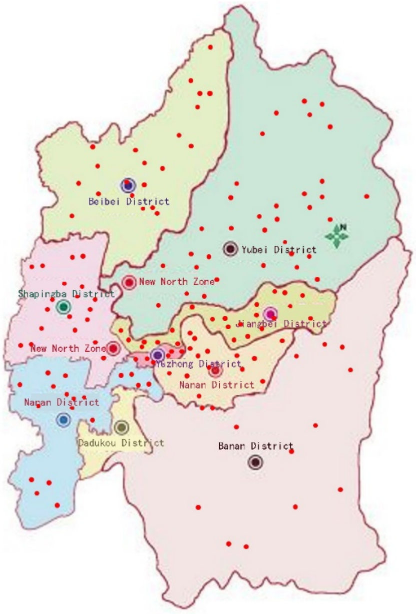

Fig. 4: Distribution of construction sites in the urban area of Chongqing.

(m^2), T represents construction time (months), EFC represents the particulate emission coefficient caused by construction sites, and is equal to emissions/(unit construction area × months). At present, the recommended EFC is $EFPM_{10}$ = 0.1061kg/m^2·month and EF_{TSP} = 0.1910 kg/ m^2·month (Li et al. 2016). Chen Min (2013) studied the size distribution of construction dust particles in the main urban area of Chongqing and found that the mass fraction of $PM_{2.5}$ was 13.29%. Therefore, the $PM_{2.5}$ emission coefficient of construction sites in the main urban area of Chongqing is calculated as $EF_{PM2.5}$ = 0.0121 kg/ m^2·month.

Selection of test objects: Preliminary investigation into the conditions of construction sites in the main urban area was necessary before conducting the field survey and monitoring. The names, geographical positions, construction stages, construction characteristics, construction scale, construction area, construction period and surrounding environment of construction sites in the study area were collected from the Chongqing Urban Construction Authority, which had conducted a field survey and a network survey. Representative construction sites were selected according to specific requirements on construction site monitoring. The final test objects were determined after further field investigation.

In this study, three construction sites in the main urban area of Chongqing were chosen as research subjects: commercial residential buildings "Jiangyulangting" (henceforth referred to as Project 1, Yuzhong District, Fig. 5), which covered an area of 600,000 m^2, and "Aoyuan City Heaven" (henceforth referred to as Project 2, Nanan District, Fig. 6)

Table 1: Constructing areas in different administrative districts.

Administrative districts	Constructing areas (unit: 10,000m^2)
Banan District	961.4465
Beibei District	1044.6822
Dadukou District	375.0296
jiangbei District	867.3437
Jiulongpo District	855.3621
Nanan District	651.85
Shapingba District	969.7696
Yubei District	1421.6378
Yuzhong District	356.5951
New North District	1553.43
High-tech District	592.2935
Economic Development Zone (south shore)	533.794
New Liangjiang District	2996.6766
Total:	13179.9107

Data source: http://jzzb.cqjsxx.com/cq_zj/

which covered an area of 526,166m^2, as well as the office building project "Guoxing Beian Jiangshan" (henceforth referred to as Project 3, Jiangbei District, Fig. 7), which covered an area of 1050,000m^2. The average release height was 3m. The purple star denotes where the test instrument was installed.

To ensure selected monitoring sites and field monitoring data were sufficiently representative, attention was paid to:

Reasonable and standard layout of monitoring sites: The area and rules of a monitoring site directly influence how the site is laid out and the results it produces. Regularly-shaped (e.g. rectangle or square) monitoring sites that did not have over-long perimeters were selected as often as possible.

Monitoring sites operated normally during the monitoring period: The recommended emission coefficients of construction sites were adjusted according to tested upwind and downwind concentrations. These were used to estimate $PM_{2.5}$ emissions caused by construction dust in the study area. Hence, the final estimation's accuracy was determined directly by whether the monitoring concentration could reflect construction dust concentration. Selected monitoring sites operated normally during the monitoring period and tried to avoid large sources of dust pollution in the surrounding areas.

Field sampling and monitoring environment were safe and operable: Since construction dust monitoring is implemented in potentially risky construction sites, the inner and surrounding environments of the construction sites were thoroughly scrutinized during monitoring site selection in order to assure the safety of test workers and monitoring operability.

Fig. 5: Project 1

Fig. 6: Project 2

Fig. 7: Project 3

Fig. 8: Test site of project 1.

Fig. 9: Test site of project 2.

Fig. 10: Test site of project 3.

Field sampling: Upwind and downwind methods were adopted in the test. It was therefore necessary to get accurate upwind and downwind net concentrations. Before monitoring, prevailing wind direction was determined according to field monitoring data. Net concentrations were then calculated according to upwind and downwind concentrations. During the sampling period, the wind mainly blew southeast. During sampling, upwind and downwind testers were

Table 2: Meteorological parameters of field test.

Date 2015	Initial sampling time	Sampling time (h)	Temperature (°C)	Wind direction	Wind speed (m/s)
4.16	12:30	4	23.6	Southeast	0.9
4.23	12:30	4	25.3	Southeast	2.8
4.30	12:30	4	27.2	Southeast	3.7
5.7	12:30	4	28.1	Southeast	0.8
5.14	12:30	4	29.7	Southeast	1.4

installed (Figs. 8, 9, 10). The sampling concentration (C) was calculated from Equation (7):

$$C = (M_2 - M_1)/V \quad ...(7)$$

Where, M_2 is the post-sampling mass (mg), M_1 is the pre-sampling mass (mg) and V is the actual sampling volume (m^3).

Field monitoring determines the upwind and downwind $PM_{2.5}$ emissions, as well as average wind speed and direction, in order to calculate variations of $PM_{2.5}$ concentration at construction sites. Hence, field sampling and monitoring in this paper mainly cover the following aspects:

$PM_{2.5}$ sample collection and concentration monitoring: Two monitoring sites were chosen at the construction sites that were upwind and downwind, respectively. The KC-120H intelligent medium-flow TSP sampler, capable of taking four levels of samples: TSP, PM10, PM5 and $PM_{2.5}$, was used. The range of the sampling flow was 80-120L/min, and sampling time and volume were accumulated automatically. At the same time, the accumulated standard sampling volume was calculated from pressure and temperature.

Weather information at 3m above the ground was monitored during the sampling period: An HP PH-SD1 wind speed and direction instrument monitored instantaneous and average wind speed and direction at the construction sites. Local atmospheric pressure, temperature, humidity, and atmospheric stability were collected from a meteorological website.

Length and width of the construction site: The length and width of the construction site were measured with tape and recorded.

Vehicle flow leaving the construction site during the field sampling and monitoring period: Since vehicle activity is an important influence on construction dust emission, recording traffic volume at the site was conducive to analysing construction dust emission.

Record sampling information: To reasonably analyse sampling results in the construction period, researchers recorded site conditions during monitoring and sampling, including construction stage, field construction machines, weather, sampling time, sampling volume, temperature, atmospheric pressure, etc.

Meteorological parameters of 3 construction sites in five experiments are listed in Table 2. All five experiments were carried out in the afternoon. Sampling time was set at 4h. Temperature increased gradually as time went on. Wind blew toward the southeast at all test times. The highest wind speed (3.7m/s) was on April 30th.

In the actual experiment, the observed dust concentration was the combined result of the construction and the road. It was therefore necessary to model a portion of the construction through an AERMOD simulation, adjust the observed value, and correct the emission parameters according to the abovementioned upwind and downwind processing method. This is shown in Fig. 11.

RESULTS AND ANALYSIS

The simulated difference between upwind and downwind concentrations, as well as the observed concentration distribution after modification, are shown in Fig. 12. The observed value is far smaller than the simulated difference. The simulated value on April 30th is about twice as high as the observed value, while the simulated values on April 16th and May 7th are closer to the observed value.

The corrected emission coefficients of the $PM_{2.5}$ mass concentration are given in Table 3. It may be observed that the corrected $PM_{2.5}$ emission coefficient in the main urban areas of Chongqing is 0.0059 kg/m^2·month. Considering A=131,799,100m^2 and T=8, the total $PM_{2.5}$ emissions are EC=A×T×EFC=6220.5t. Note that for this study, we ignored secondary particle generation caused by suspended dust.

According to experimental and estimation results, it can be observed that:

The $PM_{2.5}$ emission concentration of construction dust correlates negatively with wind speed: Based on field monitoring and data analysis, upwind and downwind net concentrations in the study area under different wind speeds were as follows: the highest average $PM_{2.5}$ concentrations were those under low wind speeds. At 0.8m/s and 0.9m/s, concentrations measured 0.0079 kg/m^2·month and 0.0065

Table 3: Corrected emission coefficients of PM2.5 mass concentration.

Date	Wind speed (m/s)	Corrected $PM_{2.5}$ emission coefficient ($kg/m^2 \cdot month$)
2015/4/16	1.4	0.0057
2015/4/23	0.8	0.0079
2015/4/30	2.8	0.0052
2015/5/7	3.7	0.0042
2015/5/14	0.9	0.0065
Mean		0.0059
Recommended emission coefficient		0.0121

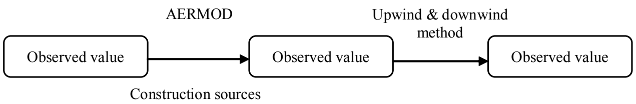

Fig. 11: Adjustment of observed value.

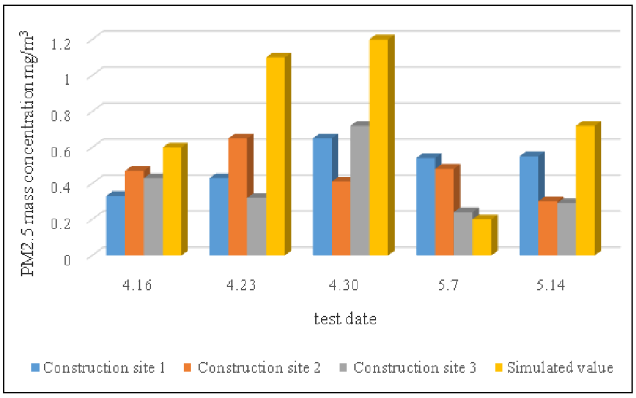

Fig. 12: Comparison between simulated difference and observed value.

$kg/m^2 \cdot month$, respectively. The average $PM_{2.5}$ concentrations under middle wind speeds were the second highest. At speeds of 1.4m/s and 2.8m/s, concentrations were 0.0057 $kg/m^2 \cdot month$ and 0.0052$kg/m^2 \cdot month$, respectively. The lowest average $PM_{2.5}$ concentration was that under high wind speed, as at a speed of 3.7m/s, concentrations only reached 0.0042$kg/m^2 \cdot month$. This is due to atmospheric conditions affecting the dilution capacity of dust.

$PM_{2.5}$ emission intensity of construction dust in the study area was low, but the total $PM_{2.5}$ emissions were very high: The present study monitored and analysed construction dust and $PM_{2.5}$ emission intensity at three representative construction sites in the main urban area of Chongqing and combined the results with related data from Chongqing Construction Quality Monitoring Information website. The resulting calculations showed that $PM_{2.5}$ emission intensity in the study area was 0.0059 $kg/m^2 \cdot month$, which was relatively higher than the recommended $PM_{2.5}$ emission intensity for construction. Additionally, the annual total $PM_{2.5}$ emissions of construction dust were extremely high at 6220.5t. This is related to the development of the construction industry and the expansive construction area. Due to the local subtropical monsoon climate, construction in the study area is not hindered by winter, and the annual average construction time can reach as high as 8 months.

CONCLUSION

$PM_{2.5}$ pollution is one of the most serious environmental problems in China, and one that much of society is trying to solve. Urban $PM_{2.5}$ pollution comes mainly from construction dust, exhaust gas emissions, and industrial emissions. Hence, effective control of $PM_{2.5}$ caused by construction dust can significantly improve the quality of urban air. To formulate effective urban $PM_{2.5}$ control measures, this paper studied the effect of construction dust on urban $PM_{2.5}$ emission characteristics by using the United States' EPA's AERMOD model to find $PM_{2.5}$ emission intensity and total emissions of construction dust. According to both results from monitoring and calculations, $PM_{2.5}$ emission intensity from construction dusts in the main urban areas of Chongqing was low, but the total $PM_{2.5}$ emissions were high due to the large scale of construction and extensive annual average construction time. Atmospheric conditions at construction sites can influence the dilution capability of construction dusts, and accordingly, $PM_{2.5}$ concentration at construction sites correlated negatively with wind speed. Effective methods for controlling urban pollution to improve air quality can be better determined by understanding construction dust's significant influence on urban $PM_{2.5}$ emissions.

The emission intensity of $PM_{2.5}$ from construction dust is influenced by many factors. Future research will focus on monitoring $PM_{2.5}$ emission concentration during different stages of construction and more accurate, scientific evaluation of the influence of construction dust on $PM_{2.5}$ emission characteristics.

ACKNOWLEDGEMENTS

The study was supported by the Social Science and Humanity on Young Fund of the Ministry of Education P.R. China (No. 15YJC630003), and Chongqing Graduate Student Research Innovation Project (No. CYB14038).

REFERENCES

Chang, C., Chang, Y. and Lin, W. et al. 2010. Fugitive dust emission source profiles and assessment of selected control strategies for particulate matter at gravel processing sites in Taiwan. Journal of the Air & Waste Management Association, 60(10): 1262-1268.

Chang, Y., Hu, W. and Su, K. et al. 2014. PM_{10} Emissions reduction from exposed areas using grass-planted covering: Field study of a construction site. Journal of Environmental Engineering, 140(6): 601-612.

Chen, M. 2013. Analysis on the distribution of PAHs in PM10 and $PM_{2.5}$ in Chongqing. Chongqing: Master Degree Thesis of Southwest University, China.

Huang, Y. M. 2006. Research on estimation and distribution characteristics of urban fugitive dust. Shanghai: Master Degree Thesis of East China Normal University, China.

Frost, K. D. 2014. AERMOD performance evaluation for three coal-fired electrical generating units in Southwest Indiana. Journal of the Air & Waste Management Association, 64 (3):280-290.

Gulia, S., Shrivastava, A. and Nema, A. et al. 2015. Assessment of urban air quality around a heritage site using AERMOD: A case study of Amritsar city, India. Environmental Modeling & Assessment, 20(6): 599-608.

Han, S., Youn, J. and Jung, Y. 2011. Characterization of PM_{10} and $PM_{2.5}$ source profiles for resuspended road dust collected using mobile sampling methodology. Atmospheric Environment, 45(20): 3343-3351.

Huang, Q., Cheng, S. Y. and Li, Y. P. et al. 2010. An integrated MM5-CAMx modeling approach for assessing PM_{10} contribution from different sources in Beijing, China. Journal of Environmental Informatics, 15(2): 47-61.

Huang, Q., Cheng, S. and Li, J. et al. 2012. Assessment of PM_{10} emission sources for priority regulation in urban air quality management using a new coupled MM5-CAMx-PSAT modeling approach. Environmental Engineering Science, 29(5): 343-349.

Kim, E. 2015. The Effect of Construction on ambient PM_{10} in the surrounding area - focusing on the field case research. Journal of Environmental Health Sciences, 41(3): 163-170.

Kong, S., Ji, Y. and Lu, B. et al. 2011. Characterization of PM_{10} source profiles for fugitive dust in Fushun-a city famous for coal. Atmospheric Environment, 45(30): 5351-5365.

Li, N., Long, X. and Tie, X. et al. 2016. Urban dust in the Guanzhong basin of China, part II: A case study of urban dust pollution using the WRF-Dust model. Science of the Total Environment, 54(1): 1614-1624.

Ni, T., Han, B. and Bai, Z. 2012. Source Apportionment of PM_{10} in four cities of Northeastern China. Aerosol and Air Quality Research, 12(4): 571-582.

Querol, X., Alastuey, A. and Viana, M. M. et al. 2004. Speciation and origin of PM_{10} and $PM_{2.5}$ in Spain. Journal Of Aerosol Science, 35(9): 1151-1172.

Ssntacatalina, M., Reche, C. and Minguillon, M. C. et al. 2010. Impact of fugitive emissions in ambient PM levels and composition A case study in southeast Spain. Science of the Total Environment, 408(21): 4999-5009.

Sik, K. Y., Choi, W. and Joong, O. K. 2009. A Study of the amount of fugitive dust generated from new harbor construction site and the prediction of effect using Aermod. Journal of Environmental Health Sciences, 35(4): 304-314.

Su, K., Chang, Y., Hu, W., Chen, S. and WU, C. et al. 2010. Comparison of reduction efficiency of woven straw for entrained emissions of particulate matter with diameters less than 10 mu m (PM_{10}) and less than 2.5 mu m ($PM_{2.5}$) from exposed areas at construction sites. Canadian Journal of Civil Engineering, 37(5): 787-795.

Tartakovsky, D., Broday, D. M. and Stern, E. 2013. Evaluation of AERMOD and CALPUFF for predicting ambient concentrations of total suspended particulate matter (TSP) emissions from a quarry in complex terrain. Environmental Pollution, 17(9): 138-145.

Tian, G., Li G., Yan B. L. and Huang, Y. H. et al. 2008. Spatial dispersion laws of fugitive dust from construction sites. Environmental Science, 1: 259-262.

Wang, T., Jiang, F. and Deng, J. et al. 2012. Urban air quality and regional haze weather forecast for Yangtze River Delta region. Atmospheric Environment, 58 (SI): 70-83.

Wang, Z., Hua, L. and Hu Y. Q. et al. 2007. Diameter distribution of particles from fugitive emission sources in Beijing. Environmental Monitoring in China, 2: 75-78.

Wen, L. L. 2011. Numerical Simulation of the Spatial Migration Rule of Fugitive Dusts at Urban Building Construction Sites. Lanzhou: Master Degree Thesis of Lanzhou University, China.

Zhao, P. S., Feng, Y. C. and Jin, J. et al. 2009. Characteristics and control indicators of fugitive dust from building construction sites. Journal of Environmental Sciences, 8: 1618-1623.

Zhao, X. Y., Cheng, S. Y. and Tian, G. et al. 2007. Construction fugitive dust pollution and control in Beijing. Journal of Beijing University of Technology, 10: 1086-1090.